Galaxy Publication

Targeting ADRB2 Signaling with 10-Gingerol Enhances the Chemotherapeutic Response to Paclitaxel in Triple-Negative Breast Cancer

Amelie Dubois[1]*, Camille Renard[1], Louis Moreau[1]

[1]Department of Pharmacognosy, Faculty of Pharmacy, Sorbonne University, Paris, France.

*E-mail ✉ amelie.dubois.fr@gmail.com

ABSTRACT

Paclitaxel is a key drug in cancer therapy, yet its clinical benefit is often constrained by pronounced toxicity and the development of resistance. 10-Gingerol (10-G), a naturally occurring ginger-derived molecule with known anti-inflammatory and antiproliferative actions, has been proposed as a potential chemosensitizer. However, its influence on the response of triple-negative breast cancer (TNBC) to paclitaxel has not been clearly defined. This work investigates whether 10-G can improve paclitaxel efficacy in TNBC and explores the mechanism responsible. A series of cell-based and animal experiments were conducted. CCK-8 assays and colony formation tests evaluated cell growth, while apoptosis was examined using flow cytometry and TUNEL staining. Protein-level changes were assessed by Western blotting and immunohistochemical analysis. Molecular docking, together with ADRB2 gene knockdown, was used to validate the interaction between 10-G and adrenoceptor Beta 2 (ADRB2). Toxicity was monitored in mice through body-weight measurements, organ coefficient analysis (kidney and spleen), and histopathology.10-G markedly boosted the responsiveness of TNBC cells to paclitaxel and amplified paclitaxel-triggered apoptosis. Computational docking and lentiviral silencing identified ADRB2 as a direct molecular target of 10-G, with 10-G binding to and suppressing its active domain. Loss of ADRB2 reduced TNBC cell proliferation and weakened the sensitizing influence of 10-G on paclitaxel treatment. Protein analyses indicated that 10-G mediated both growth inhibition and enhanced chemotherapy response by suppressing the ADRB2/ERK cascade. Toxicity studies showed that combining 10-G with paclitaxel did not aggravate liver or kidney injury. The findings support the potential use of 10-G as an adjuvant agent to strengthen paclitaxel-based treatment in TNBC and highlight ADRB2 as a promising target for improving chemotherapy sensitivity.

Keywords: Triple-negative breast cancer, Combination treatment, 10-Gingerol, Paclitaxel, ADRB2

Introduction

Breast cancer continues to be the most prevalent malignancy diagnosed among women globally and remains a leading cause of cancer-related mortality [1]. Triple-negative breast cancer (TNBC), characterized by the absence of ER, PR, and HER2 expression, represents the most aggressive form of the disease [2], with a clinical profile marked by high recurrence rates and poor prognosis [3]. Due to the lack of effective molecular targets, chemotherapy is still the principal treatment strategy for managing TNBC [4]. Paclitaxel, a cytotoxic agent widely applied across multiple cancer types including TNBC, is regarded as a first-line drug because of its potent tumor-suppressive activity [5]. Nonetheless, the development of paclitaxel resistance significantly restricts its therapeutic efficacy [6], highlighting the urgent need for safer and more effective adjuvant agents capable of strengthening chemotherapy responses and improving clinical outcomes in TNBC.

Extensive research has indicated that naturally derived plant compounds and bioactive phytochemicals can enhance the therapeutic performance of conventional chemotherapeutics [7–9]. Ginger, commonly consumed both as a culinary ingredient and dietary supplement, is a notable source of such compounds [10]. Among its active constituents, 10-gingerol (10-G) is a major pungent molecule with documented anti-inflammatory, antioxidant,

and antiproliferative properties [11]. Compared with other gingerol analogs, 10-G exhibits the strongest antitumor potential and has been shown to induce apoptosis in several cancer cell types, including breast cancer [12, 13]. As a relatively safe natural product, 10-G has also been reported to enhance the anticancer efficacy of doxorubicin in TNBC models [14]. However, no study has yet clarified whether 10-G can modulate paclitaxel sensitivity in TNBC or elucidated the mechanisms involved.

Network pharmacology analysis suggests that adrenoceptor Beta 2 (ADRB2) may serve as a key molecular target for the antitumor effects of 10-G in TNBC [15]. ADRB2 encodes the β_2-adrenergic receptor, a member of the G protein-coupled receptor (GPCR) superfamily, and has been implicated in the progression of multiple cancers [16, 17]. Evidence indicates that ADRB2 influences chemotherapeutic responsiveness and may correlate with clinical outcomes in several malignancies [18, 19]. In breast cancer specifically, ADRB2 inhibition has been associated with reduced metastatic potential and recurrence risk [20, 21]. Additionally, findings in hepatocellular carcinoma demonstrate that silencing ADRB2 enhances the antitumor activity of sorafenib [22], further supporting the therapeutic relevance of this target. Thus, interfering with ADRB2 signaling may represent a viable strategy for improving paclitaxel efficacy in TNBC.

In this study, we demonstrate that 10-G substantially increases the therapeutic effect of paclitaxel in TNBC. ADRB2 emerges as a central mediator of the action of 10-G, and the enhancement of paclitaxel sensitivity is shown to depend on suppression of the ADRB2/ERK signaling axis. Both in vitro and in vivo evaluations confirm that 10-G does not produce measurable toxicity in mammary epithelial cells or major organs in mice. These findings provide insight into the mechanistic basis of the anticancer properties of 10-G and suggest its promise as a chemotherapeutic sensitizer for TNBC treatment.

Reagents and antibodies

The study utilized the following primary antibodies: Bcl-2 (Abcam, Cambridge, UK; ab182858), Bax (Cell Signaling Technology, Danvers, MA; 2772), cleaved-PARP (Cell Signaling Technology; 5625), ADRB2 (Proteintech, Wuhan, China; 13096-1-AP), ERK (Abcam; ab17942), phospho-ERK1/2 (Abcam; ab201015), Ki67 (Abcam; ab16667), and β-actin (Proteintech; 66009-1-Ig). Secondary antibodies included HRP-conjugated goat anti-rabbit IgG (Proteintech; SA00001-2) and HRP-conjugated goat anti-mouse IgG (Proteintech; SA00001-1).

10-Gingerol (10-G) was obtained from Chengdu Ruifensi Biotechnology Co., Ltd. (Chengdu, China). A 40 mM stock solution was prepared in dimethyl sulfoxide (DMSO; Sigma-Aldrich, Merck KGaA). The compound has a molecular formula of $C_{21}H_{34}O_4$, with its chemical structure presented in **Figure 1**. Paclitaxel (injectable formulation) was sourced from Hainan Quanxing Pharmaceutical Co., Ltd.
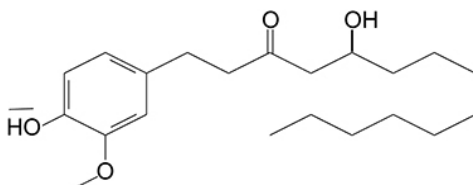

Figure 1. The structural formula of 10-G.

Cell culture

Human triple-negative breast cancer (TNBC) cell lines MDA-MB-231 and SUM-159, along with the non-malignant breast epithelial line MCF-10A, were obtained from the American Type Culture Collection (ATCC, Manassas, VA). MDA-MB-231 cells were maintained in DMEM, whereas SUM-159 cells were grown in RPMI-1640. Both media were supplemented with 10% fetal bovine serum and antibiotics (100 U/mL penicillin and 100 µg/mL streptomycin; Gibco Life Technologies, Lofer, Austria).

MCF-10A cells were cultured in DMEM enriched with 5% horse serum, antibiotics at the same concentrations as above (Gibco Life Technologies, Gaithersburg, MD), and additional supplements including recombinant human EGF (20 ng/mL), hydrocortisone (0.5 µg/mL), cholera toxin (100 ng/mL), and insulin (10 µg/mL; Sigma-Aldrich, Shanghai, China). All cell lines were incubated at 37 °C in a humidified 5% CO_2 environment.

Cell viability and combination analysis

Cells were plated at 2,000 cells per well in 96-well plates and allowed to adhere for 12 h. They were subsequently exposed to graded concentrations of 10-G (0–800 µM) and/or paclitaxel (0–1600 nM) for 48 h. Cell viability was

then assessed by adding 10 μL of the Cell Counting Kit-8 reagent to each well, followed by a 4-h incubation. Absorbance at 450 nm was measured using a Bio-Rad Model 550 microplate reader (CA). Combination effects were quantified using Compusyn (Computusyn Inc.), where CI values between 0.9–1.1 signify additive interactions, 0.3–0.9 indicate synergy, <0.3 strong synergy, and >1.1 antagonism. IC_{50} values were determined using GraphPad Prism 8.

Colony formation assay
A total of 800 cells were seeded into six-well plates and cultured for 24 h prior to treatment. Cells were then exposed to 10-G (100 μM) and/or paclitaxel (100 nM) in complete medium for 14 days. Colonies were fixed with 4% paraformaldehyde for 1 h, stained with crystal violet (Beyotime, Jiangsu, China) for 20 min, rinsed with PBS for 10 min, and air-dried. Colony numbers were quantified using ImageJ software (ImageJ 1.53e, Maryland, USA).

Cell apoptosis analysis
Apoptosis was detected using flow cytometry combined with an Annexin V-FITC/PI detection kit (Beyotime, Jiangsu, China). Approximately 2×10^5 cells were seeded into each well of a six-well plate and treated with the indicated concentrations of 10-G and paclitaxel, either alone or in combination, for 24 h during the exponential growth phase.
Staining was performed following the manufacturer's instructions. Data acquisition and analysis were carried out using NovoExpress 1.4.1 (ACEA Bioscience; Agilent Technologies). Early-stage apoptotic cells were positive for Annexin V-FITC but negative for PI, whereas double-positive cells were classified as late-stage apoptotic. PI-positive but Annexin V-negative cells were considered non-viable. Apoptosis rate was defined as the sum of early and late apoptotic percentages. Results represent the mean of three independent experiments.

Western blotting
MDA-MB-231 and SUM-159 cells in logarithmic growth were assigned to six treatment groups: control, 10-G (50 μM), 10-G (100 μM), paclitaxel alone, paclitaxel plus 10-G (50 μM), and paclitaxel plus 10-G (100 μM). Cells (2×10^5 per well) were seeded into six-well plates and treated 24 h later with the respective media. After another 24 h, cells were harvested and lysed using RIPA buffer (Sigma-Aldrich, St. Louis, MO). Total protein was quantified using a BCA kit (Beyotime, Jiangsu, China).
Western blotting procedures followed established protocols [23]. Proteins (20 μg per sample) were resolved on 10% SDS-PAGE gels and transferred to PVDF membranes (0.45 μm; Millipore, MA, USA). After blocking in 5% milk for 1 h, membranes were incubated overnight at 4 °C with primary antibodies against Bcl-2, Bax, cleaved-PARP, ADRB2, ERK, phospho-ERK1/2, and β-actin (all 1:1000). ERK and β-actin served as loading controls. After washing, HRP-conjugated anti-rabbit or anti-mouse secondary antibodies (1:5000) were applied for 1 h at room temperature. Bands were visualized using ECL reagents (Tanon Science & Technology, Shanghai, China) and imaged with ChemiDoc TMXRS+ (Bio-Rad, USA). Band intensities were quantified with ImageJ 1.53e.

Generation of stable ADRB2-shRNA cell lines
ADRB2 knockdown was achieved via lentiviral transduction using ADRB2-shRNA constructs (**(Table 1)**; Shanghai Gikegien Technology Co., Ltd.). MDA-MB-231 and SUM-159 cells (2×10^5 per well) were seeded into six-well plates and infected the following day at MOIs of 50 and 20, respectively. After infection, cells underwent puromycin selection (1 mg/mL) for approximately 1 week to establish stable knockdown lines. Successful silencing of ADRB2 expression was confirmed by Western blotting.

Table 1. The shRNA sequence of lentiviruses

NO.	Target Sequences
Control-shRNA	TTCTCCGAACGTGTCACGT
ADRB2-shRNA	GCCATTACTTCACCTTTCAAG

Molecular docking
The molecular structure of 10-G was drawn using ChemDraw Professional 15.1 (PerkinElmer, USA). The crystal structure of ADRB2 (PDB ID: 3NYA) was retrieved from the RCSB Protein Data Bank. Docking simulations

were then carried out in Accelrys Discovery Studio 3.5 (Accelrys Inc., USA) following established procedures [24].

Breast cancer xenografts in NOD/SCID mice

Female NOD/SCID mice (five weeks old, 19 ± 0.5 g) were supplied by the Experimental Animal Centre of Southern Medical University. Animals were maintained under SPF conditions (25 °C, 40–60% humidity, 12-h light/dark cycle) with unrestricted access to chow and filtered water, and allowed to acclimate for one week prior to experimentation. Ethical approval for all procedures was granted by the Guangdong Provincial Hospital of Chinese Medicine (Reference No. 2020031). All animal handling complied with the Institutional Animal Ethical Committee (IAEC) requirements and the *Guide for the Care and Use of Laboratory Animals* (2011).

To induce xenografts, each mouse received an injection of MDA-MB-231 cells (5×10^6 cells in 200 μL PBS) into the mammary fat pad. Tumor growth was measured with digital calipers beginning on day 3. Four days after inoculation, mice were randomized based on tumor size—using the RAND function in Microsoft Excel—into four treatment groups (n = 5): vehicle, 10-G (40 mg/kg), paclitaxel (10 mg/kg), and combined paclitaxel (10 mg/kg) + 10-G (40 mg/kg), using a method similar to Schvarcz *et al*. [25].

The vehicle group received 0.5% CMC-Na and saline. 10-G was administered orally once daily in 0.5% CMC-Na, whereas paclitaxel was diluted in saline and given every three days. Body weight was monitored throughout the study. Tumor volume was calculated every three days using the formula:

$$\text{tumor volume} = (\text{length} \times \text{width}^2) / 2 \tag{1}$$

On day 33, animals were euthanized via CO_2 asphyxiation followed by cervical dislocation. Tumors, livers, and kidneys were excised and weighed. Organ indices were calculated as:

$$\text{liver coefficient} = (\text{liver mass/body weight}) \times 100\%, \tag{2}$$

$$\text{kidney coefficient} = (\text{kidney mass/body weight}) \times 100\%, \tag{3}$$

which were used to evaluate systemic toxicity.

Immunohistochemistry and TUNEL assay

Tumor tissues were fixed in 4% paraformaldehyde for 24 h, processed through routine dehydration and paraffin embedding, and cut into 4-μm sections. After drying, sections were deparaffinized in xylene and rehydrated through graded ethanol solutions. Immunohistochemistry was performed as described previously [26]. Primary antibodies were applied at the following dilutions: Bcl-2 (1:500), Bax (1:200), cleaved-PARP (1:100), ADRB2 (1:200), phospho-ERK1/2 (1:1000), and Ki-67 (1:100). Staining quality reagents of analytical grade were used throughout. Images were obtained using a BX51 light microscope (Olympus) at 10× magnification, and three randomly selected fields per sample were evaluated independently by pathologists.

TUNEL staining followed the procedure reported by Zheng *et al*. [27]. Briefly, tissue sections were dewaxed, incubated with proteinase K at 37 °C for 30 min, and then treated with TUNEL working solution (Beyotime, Jiangsu, China) for 1 h at 37 °C. After PBS washing, nuclei were counterstained with DAPI for 5 min. Fluorescence signals were visualized using excitation at 450–500 nm and emission at 515–565 nm on an Olympus BX51 microscope.

Haematoxylin and eosin staining

Tissues were fixed in 4% paraformaldehyde for 24 h, embedded in paraffin, and sectioned at 4 μm. Standard histological staining with hematoxylin and eosin was performed. Slides were examined under 10× magnification (Olympus BX51) to evaluate liver and kidney morphology.

Statistical analysis

Continuous variables are presented as mean (SD) or median (range), and categorical variables as frequency (percentage). Comparisons between two groups were made using independent-samples t-tests (for normally distributed variables) or Mann–Whitney U-tests (for non-normal distributions). For comparisons across three or more groups, one-way ANOVA or Welch's ANOVA was applied as appropriate. Post-hoc testing consisted of

Tukey's test (equal variances), Dunnett's T3 (unequal variances), or Dunn–Bonferroni (non-parametric). All statistical analyses were performed in SPSS 26.0 (SPSS Inc., Chicago, IL).

Results and Discussion

10-G Suppresses Proliferation, Reduces Colony Formation, and Enhances Paclitaxel Sensitivity in TNBC Cells
To assess whether 10-G modulates paclitaxel responsiveness, TNBC cell lines MDA-MB-231 and SUM-159 were treated with increasing concentrations of 10-G and/or paclitaxel for 48 h **(Figure 2a).** The IC_{50} values of 10-G were 139.39 μM for MDA-MB-231 and 195.42 μM for SUM-159, while paclitaxel IC_{50} values were 294.70 nM and 336.18 nM, respectively **(Table 2)**. As demonstrated in **Figure 2a**, 10-G inhibited TNBC cell growth in a concentration-dependent manner. CI analysis revealed a synergistic interaction between 10-G and paclitaxel (CI < 1).

Low-dose paclitaxel (100 nM) combined with 10-G markedly increased growth inhibition **(Figure 2c)**. In contrast, the non-tumorigenic epithelial line MCF-10A exhibited a much higher IC_{50} for 10-G (619.83 μM), and 10-G did not potentiate paclitaxel cytotoxicity in these cells **(Figure 2b)**.

Clonogenic assays further confirmed the CCK-8 results: treatment with 10-G (100 μM), paclitaxel (100 nM), or the combination significantly reduced colony numbers, with the co-treatment group showing the greatest reduction (**Figure 2d**, P < 0.05).

Collectively, these data indicate that 10-G effectively inhibits TNBC cell proliferation and augments sensitivity to paclitaxel in a dose-dependent manner.

Table 2. The drug IC50 value of MDA-MB-231, SUM-159 and MCF-10A cells treated with different concentrations of 10-G or paclitaxel for 48 h

Cell	Drug IC50	
	10-G (μM)	Taxol (nM)
MDA-MB-231	139.39 (124.65–154.13)	294.70 (182.38–407.02)
SUM-159	195.42 (152.25–238.59)	336.18 (265.47–406.89)
MCF-10A	619.83 (477.21–762.44)	471.12 (377.03–565.21)

Abbreviations: TNBC, triple-negative breast cancer; 10-G, 10-gingerol; CCK8, cell counting kit 8; GPCRs, G protein-coupled receptor; CI, combined index; IC50, The half-maximal [50%] inhibitory concentration.
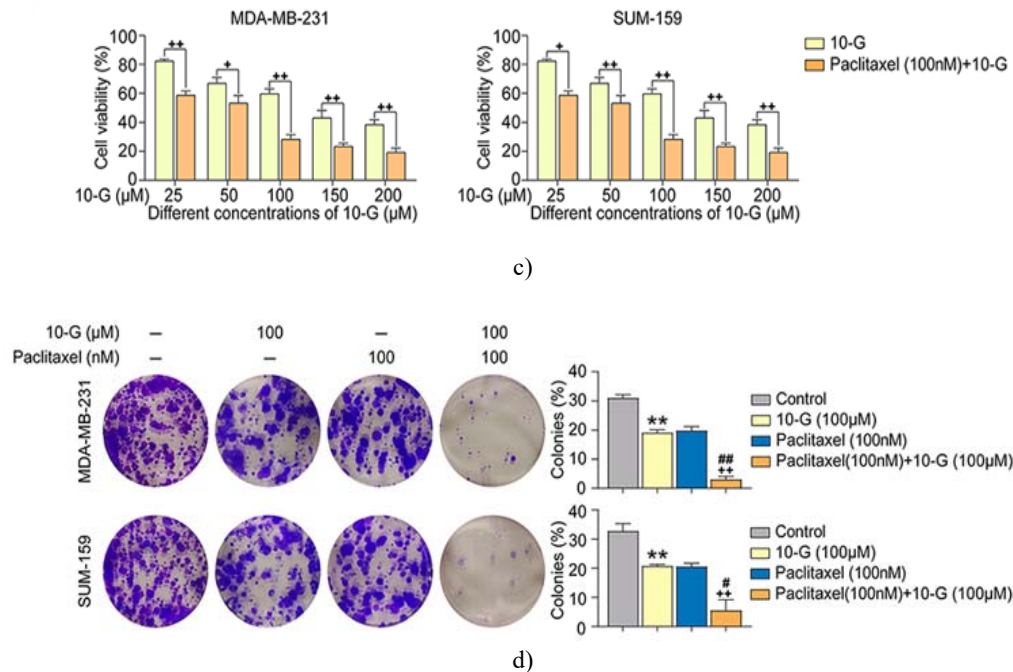

a)

b)

c)

d)
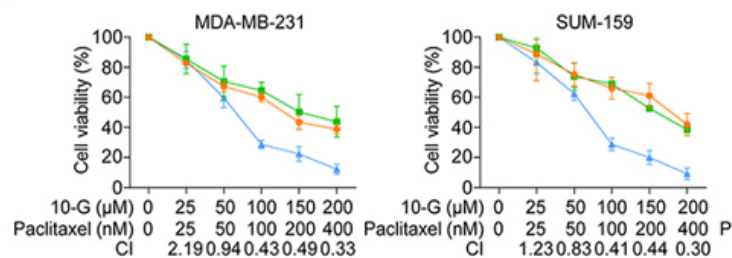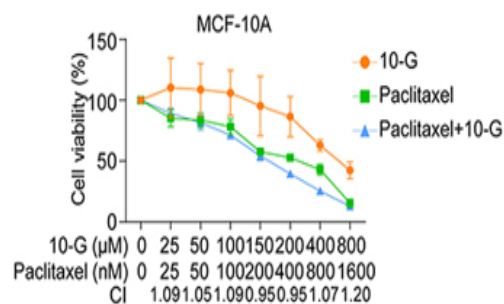
Figure 2. 10-G enhances the inhibitory effects of paclitaxel on TNBC cell proliferation and colony growth.
(a, b) MDA-MB-231, SUM-159, and the non-malignant epithelial line MCF-10A were exposed to increasing concentrations of 10-G or paclitaxel, either individually or in combination, for 48 h. Cell viability was quantified using the CCK-8 assay. Drug interaction was assessed using the Combination Index (CI) calculated via Compusyn.
(c) Proliferation of TNBC cells following treatment with escalating doses of 10-G together with paclitaxel (100 nM) for 48 h.
(d) Representative colony-formation images of TNBC cells after exposure to 10-G, paclitaxel, or their combination.
Data are expressed as mean ± SD. **$P < 0.01$ vs. control; ##$P < 0.01$ vs. paclitaxel alone; +$P < 0.05$, ++$P < 0.01$ vs. 10-G alone.
Abbreviations: 10-G, 10-gingerol; TNBC, triple-negative breast cancer.

10-G synergistically enhances paclitaxel-induced apoptosis

Given the observed growth-inhibitory and chemosensitizing effects of 10-G on TNBC cells, we next examined whether these outcomes were associated with apoptotic induction. MDA-MB-231 and SUM-159 cells were treated with varying concentrations of 10-G and/or paclitaxel for 48 h, followed by flow-cytometric evaluation of apoptotic populations. As shown in **Figures 3a and 3b**, 10-G alone significantly increased apoptosis in a dose-dependent manner ($P < 0.05$). Co-treatment with paclitaxel further amplified apoptotic cell fractions compared with paclitaxel monotherapy ($P < 0.05$).

Consistent with these findings, 10-G exposure for 48 h elevated Bax and cleaved-PARP expression while suppressing Bcl-2 levels (**Figures 3c and 3d**, $P < 0.05$). These molecular alterations were even more pronounced when 10-G was combined with paclitaxel ($P < 0.05$).

Together, these results indicate that 10-G potentiates the apoptotic response induced by paclitaxel, likely by reinforcing mitochondrial-mediated apoptosis signaling in TNBC cells.
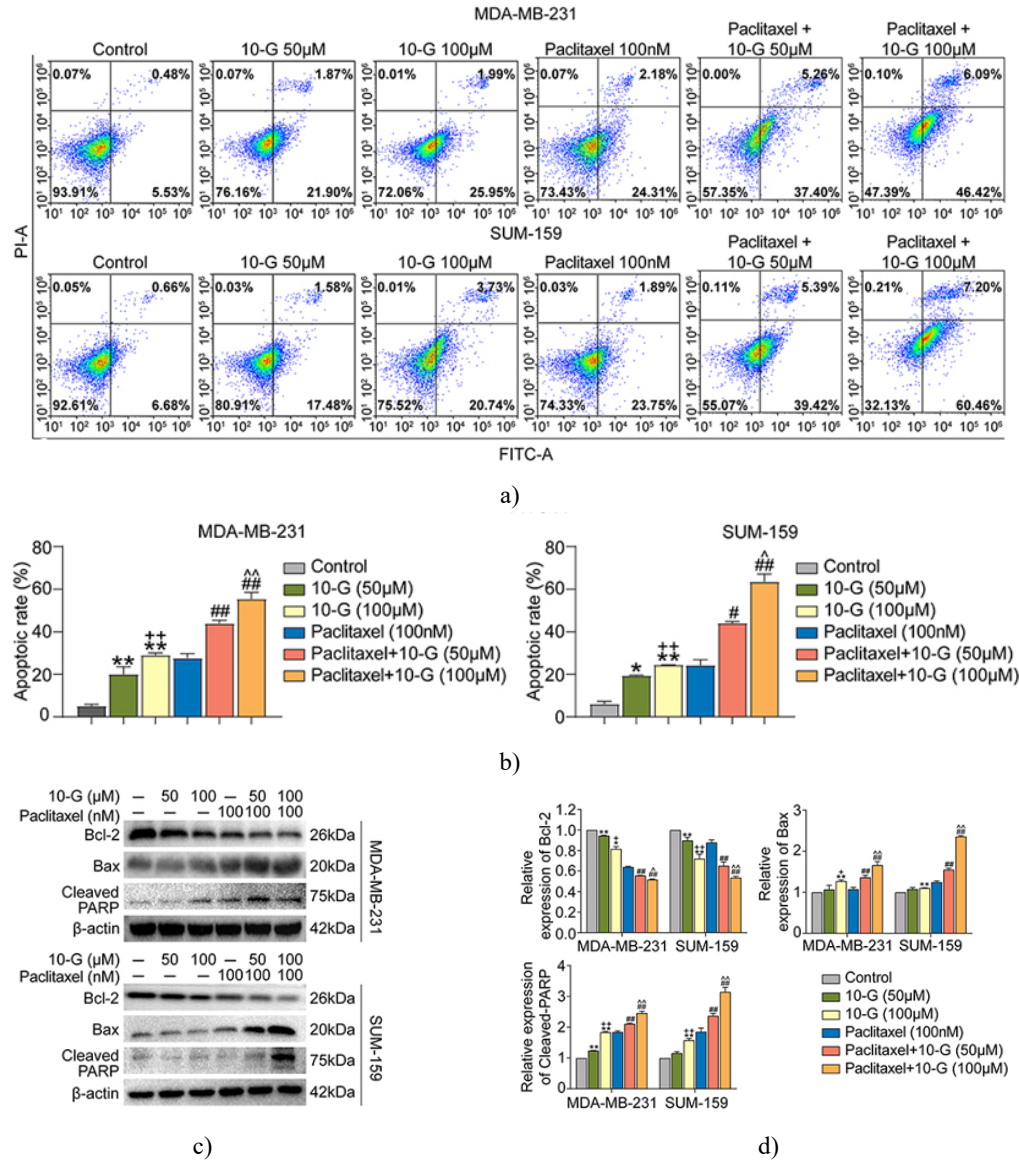
a)

b)

c)   d)

Figure 3. 10-G enhances apoptosis in TNBC cells, alone and in combination with paclitaxel.
(a) MDA-MB-231 and SUM-159 cells were treated for 24 h with 10-G, paclitaxel, or their combination.
Apoptosis was assessed using Annexin V-FITC/PI dual staining.
(b) Quantification of apoptotic percentages in both TNBC cell lines.
(c, d) Protein levels of Bcl-2, Bax, and cleaved-PARP were determined by Western blot after 24 h of the indicated treatments.
Data are presented as mean $\pm$ SD. *$P < 0.05$, **$P < 0.01$ vs. control; +$P < 0.05$, ++$P < 0.01$ vs. 10-G (50 μM);
#$P < 0.05$, ##$P < 0.01$ vs. paclitaxel; ^$P < 0.05$, ^^$P < 0.01$ vs. paclitaxel + 10-G (50 μM).
Abbreviations: 10-G, 10-gingerol; TNBC, triple-negative breast cancer.

10-G interacts with ADRB2 to inhibit tumor growth and enhance chemotherapy
To investigate whether ADRB2 mediates the chemosensitizing effect of 10-G, molecular docking was performed. The binding energy between 10-G and ADRB2 was calculated as −7.7 kcal/mol. Docking results revealed that 10-G fits within the active site of ADRB2, forming hydrogen bonds with TYR-316, ASN-312, and SER-203, and engaging in hydrophobic interactions with TRP-313, PHE-290, VAL-114, and VAL-117 **(Figure 4a).**
To validate these interactions, MDA-MB-231 and SUM-159 cells were transfected with lentiviral vectors encoding either ADRB2 shRNA or control shRNA **(Figure 4a).** Knockdown of ADRB2 significantly reduced cell proliferation and colony formation, as shown by CCK-8 and clonogenic assays **(Figures 4b and 4c**, $P < 0.05$).

Notably, the ability of 10-G to inhibit tumor growth and sensitize cells to paclitaxel was attenuated following ADRB2 silencing **(Figures 4b and 4c**, P < 0.05). These findings indicate that ADRB2 is a critical molecular target through which 10-G mediates its anti-cancer and chemotherapy-enhancing effects.
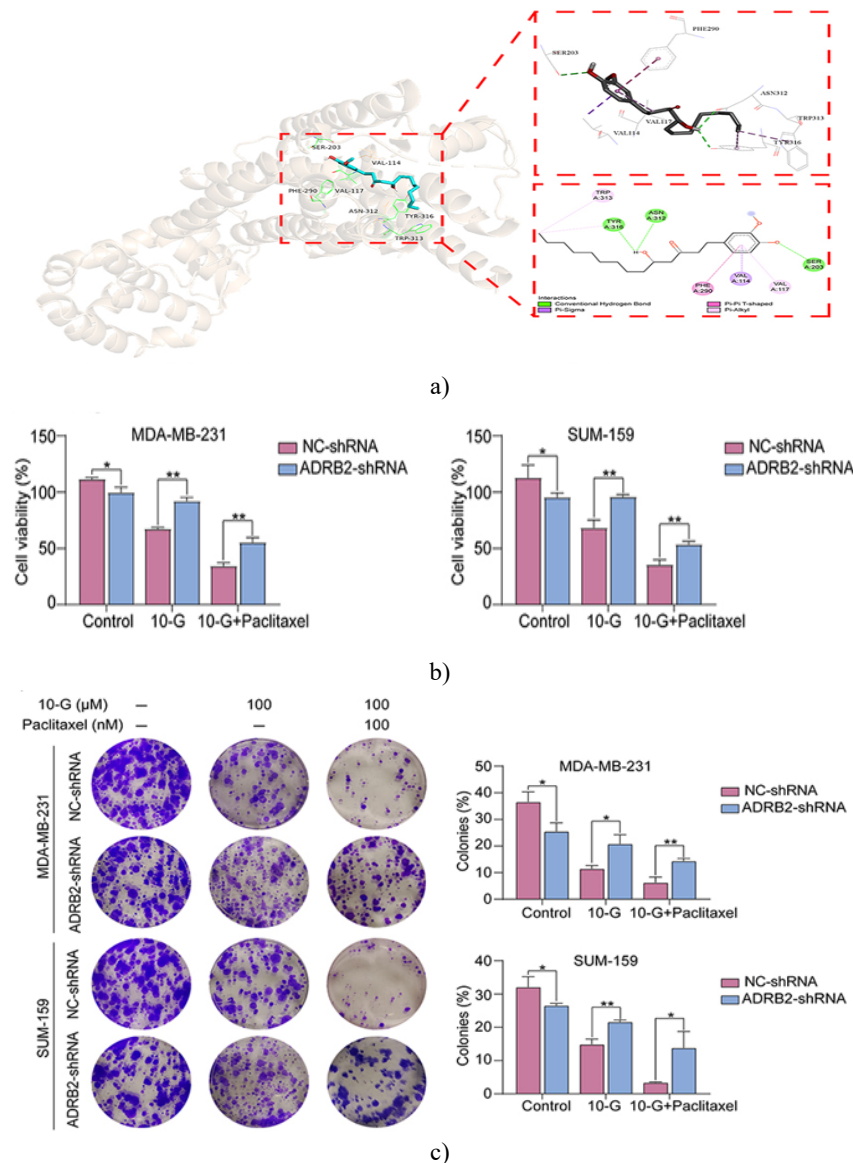

a)

b)

c)

Figure 4. ADRB2 is a critical molecular target for 10-G activity.
(a) Molecular docking of 10-G within the active site of ADRB2, showing hydrogen bonding and hydrophobic interactions.
(b) MDA-MB-231 and SUM-159 cells were transfected with either control (NC) or ADRB2-shRNA lentivirus for 48 h, followed by treatment with varying concentrations of 10-G, paclitaxel, or their combination for 48 h. Cell viability was measured using the CCK-8 assay.
(c) Colony formation of TNBC cells was assessed after ADRB2 knockdown. ADRB2 silencing reduced colony numbers and attenuated the cytotoxic effects of 10-G.
Data are expressed as mean ± SD. *P < 0.05, **P < 0.01 vs. NC-shRNA.
Abbreviations: 10-G, 10-gingerol; TNBC, triple-negative breast cancer.

10-G potentiates paclitaxel efficacy by suppressing ADRB2/ERK signaling
ADRB2 functions as an upstream regulator of ERK, and its aberrant activation contributes to tumor progression and chemoresistance [28]. To evaluate the relationship between ADRB2 and ERK phosphorylation, TNBC cells

transfected with ADRB2 shRNA or control shRNA were analyzed. Western blotting demonstrated that ADRB2 knockdown significantly decreased p-ERK1/2 levels, indicating reduced ERK activation (**Figures 5a and 5b**, P < 0.05).

Next, we examined the effects of 10-G and paclitaxel on ADRB2 and ERK signaling. Treatment with 10-G alone reduced ADRB2 and p-ERK1/2 expression in a dose-dependent manner in both MDA-MB-231 and SUM-159 cells (**Figures 5c and 5d**, P < 0.05). Co-treatment with 10-G and paclitaxel led to further suppression of these proteins (P < 0.05). These results suggest that 10-G enhances paclitaxel-mediated growth inhibition in TNBC cells through downregulation of the ADRB2/ERK signaling pathway.
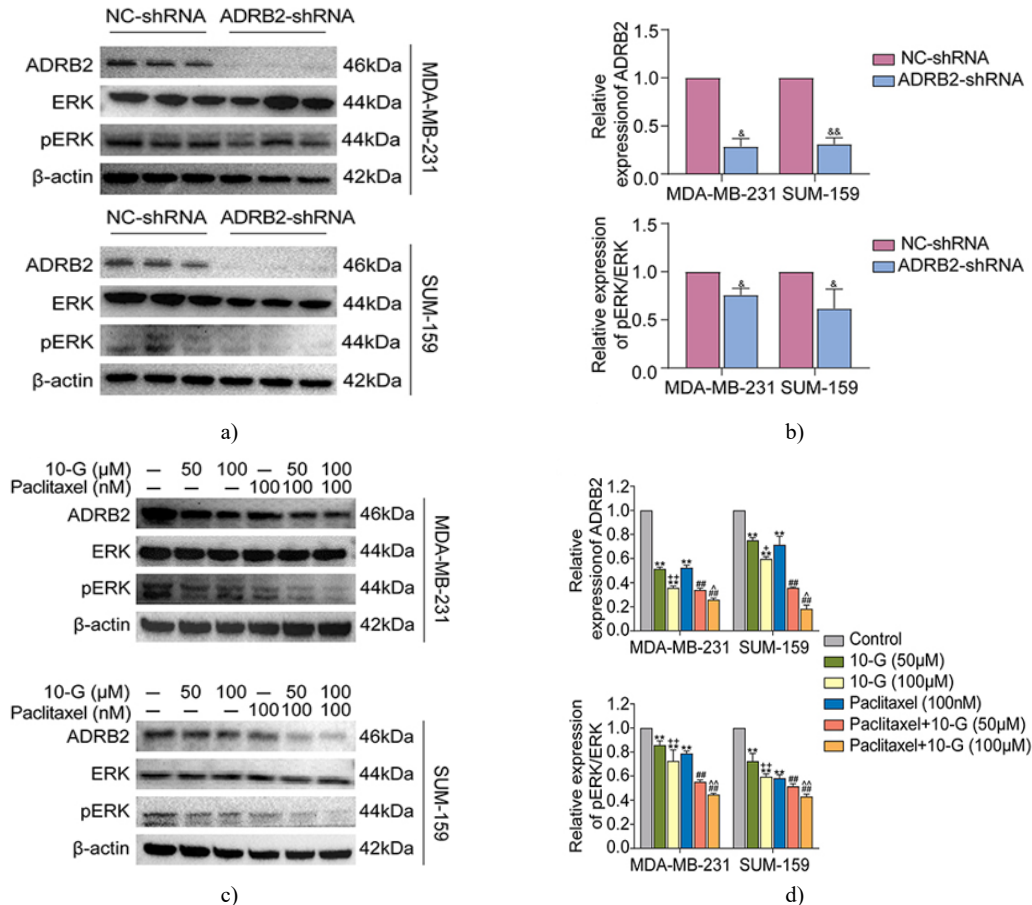

Figure 5. 10-G enhances paclitaxel-mediated inhibition of ADRB2/ERK signaling.
(a, b) Expression levels of total ERK and phosphorylated ERK in TNBC cells following ADRB2 knockdown via lentiviral shRNA.
(c, d) MDA-MB-231 and SUM-159 cells were treated for 24 h with 10-G, paclitaxel, or their combination. ADRB2, total ERK, and p-ERK protein levels were assessed by Western blot.
Data are expressed as mean ± SD. &P < 0.05, &&P < 0.01 vs. NC-shRNA; **P < 0.01 vs. control; +P < 0.05, ++P < 0.01 vs. 10-G (50 μM); ##P < 0.01 vs. paclitaxel; ^P < 0.05, ^^P < 0.01 vs. paclitaxel + 10-G (50 μM)..
Abbreviations: 10-G, 10-gingerol; TNBC, triple-negative breast cancer

10-G enhances paclitaxel anti-tumor activity in a TNBC xenograft model
The in vivo anti-tumor effects of 10-G alone and in combination with paclitaxel were evaluated using MDA-MB-231 xenografts in NOD/SCID mice. Tumor-bearing mice received oral 10-G at 40 mg/kg based on pre-experiment optimization. Both 10-G and paclitaxel monotherapies significantly reduced tumor growth compared with vehicle-treated controls **(Figures 6a and 6b)**. Notably, combined treatment produced the most pronounced tumor suppression.

TUNEL assays and analysis of apoptosis-associated proteins (cleaved-PARP, Bax, and Bcl-2) revealed that both agents, individually or together, increased apoptotic activity in tumor tissues **(Figure 6c).** Immunohistochemical

staining for Ki67 demonstrated reduced proliferative activity following either treatment, with the greatest effect observed in the combination group.

Furthermore, 10-G significantly decreased ADRB2 and p-ERK1/2 expression in tumor tissues, and this effect was further enhanced when combined with paclitaxel **(Figure 6c)**, consistent with the in vitro findings. These results indicate that 10-G potentiates paclitaxel-induced tumor suppression by activating apoptosis and inhibiting ADRB2/ERK signaling, thereby limiting tumor growth in vivo.
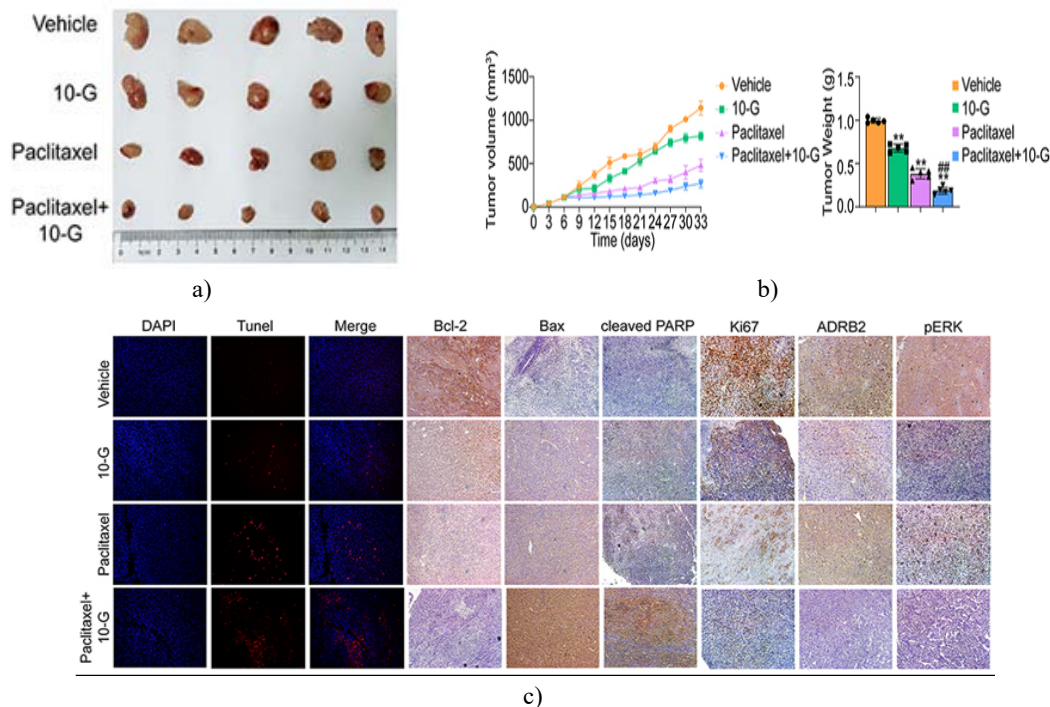

Figure 6. 10-G potentiates the anti-tumor effects of paclitaxel in vivo.

(a) Representative images of tumors from each treatment group (n = 5).

(b) Tumor volumes were measured every three days, and tumor weights were recorded at the end of the experiment (n = 5).

(c) Representative DAPI/TUNEL double-staining images showing apoptotic cells in tumor tissues from each group (n = 5).

(d) Immunohistochemical analysis of Ki67, ADRB2, p-ERK, Bcl-2, Bax, and cleaved-PARP in tumor sections (n = 5).

Data are presented as mean ± SD. **P < 0.01 vs. vehicle; ##P < 0.01 vs. paclitaxel. Magnification, ×100. Abbreviation: 10-G, 10-gingerol.

Toxicity assessment

To evaluate potential in vivo toxicity, mice were monitored for 30 days. Treatment with 10-G alone did not cause significant body weight changes, while paclitaxel monotherapy induced slight weight loss. Co-administration of 10-G with paclitaxel did not exacerbate this effect **(Figure 5b)**. No adverse signs, including skin lesions, diarrhea, or treatment-related mortality, were observed during the study.

Histopathological examination of liver and kidney tissues using H&E staining revealed no morphological abnormalities in the 10-G-treated mice compared with vehicle controls **(Figures 7a and 7b)**. Additionally, liver and kidney indices showed no significant differences across the treatment groups **(Figures 7a and 7b)**. These results indicate that 10-G exhibits a favorable safety profile in vivo.
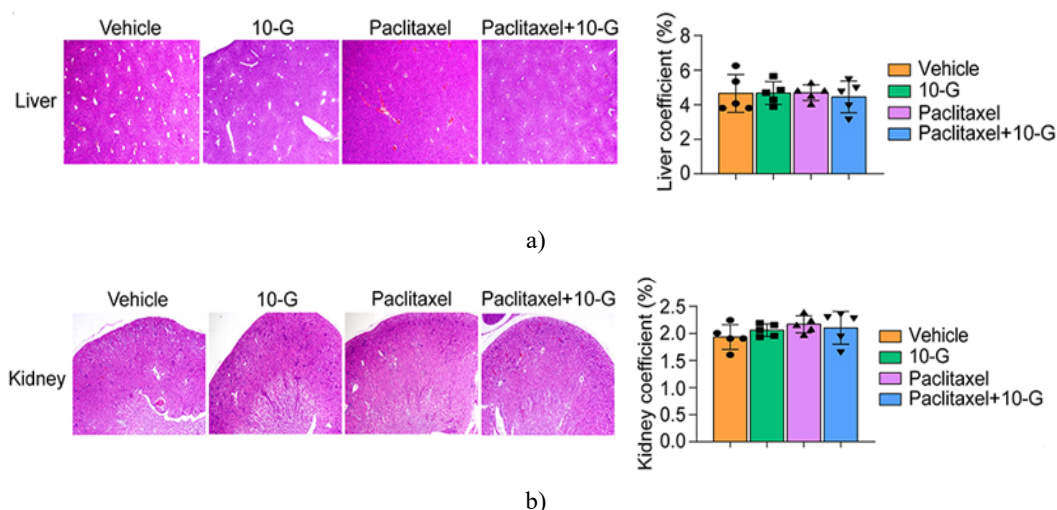
a)

b)

Figure 7. 10-G shows no significant pathological effects on liver and kidney tissues.
(a) Representative H&E-stained liver sections and corresponding liver coefficients across treatment groups.
(b) Representative kidney H&E images and kidney coefficients for each group.
Data are presented as mean ± SD. Magnification, ×100.
Abbreviation: 10-G, 10-gingerol.

Triple-negative breast cancer (TNBC) is an aggressive malignancy with high metastatic potential. Chemotherapy remains the primary therapeutic approach, but long-term paclitaxel treatment often leads to drug resistance and tumor recurrence. Combining chemotherapy with synergistic agents may allow dose reduction, minimize side effects, and delay resistance, representing a promising strategy to enhance treatment outcomes [29]. Among natural compounds, 10-gingerol (10-G) has emerged as a potential anti-cancer agent due to its anti-inflammatory and anti-tumor properties [30, 31]. Our study demonstrates that 10-G increases TNBC cell sensitivity to paclitaxel and elucidates its underlying molecular targets and mechanisms.

Apoptosis plays a critical role in tumor suppression. Previous studies have shown that 10-G can induce apoptosis in breast cancer cells [32], consistent with our findings. In vitro, 10-G inhibited TNBC cell growth in a dose-dependent manner and promoted apoptosis, effects that were markedly enhanced when combined with paclitaxel. These results confirm that the anti-tumor and chemosensitizing properties of 10-G are closely linked to apoptosis induction.

Network pharmacology and bioinformatics analysis identified ADRB2 as a potential target of 10-G [15], and molecular docking confirmed its interaction. Both in vitro and in vivo experiments revealed that 10-G suppresses ADRB2 expression in a dose-dependent manner, and ADRB2 knockdown reduced TNBC proliferation and colony formation, supporting its role as a mediator of 10-G's effects. Interestingly, paclitaxel alone also reduced ADRB2 expression, but its anti-tumor activity was not impaired following ADRB2 silencing, consistent with clinical data showing that combining ADRB2 blockers with paclitaxel does not diminish efficacy or increase patient risk [33]. These observations suggest that ADRB2 is a specific target for 10-G rather than for paclitaxel. Targeting ADRB2 may therefore offer a new approach to enhance chemotherapy efficacy.

ADRB2 regulates multiple signaling pathways, including ERK, which is involved in proliferation, apoptosis, and chemotherapy resistance [34–38]. Phosphorylation of ERK is crucial for its activation and contributes to breast cancer progression [39]. Consistent with prior findings [40], ADRB2 knockdown blocked ERK phosphorylation in TNBC cells. Suppressing p-ERK1/2 has been reported to improve paclitaxel efficacy [41, 42], highlighting ADRB2/ERK as a key therapeutic axis. In our study, treatment with 10-G alone or in combination with paclitaxel significantly reduced ERK phosphorylation in a dose-dependent manner. Previous research also supports that 10-G can induce mitochondrial apoptosis by inhibiting ERK signaling [43]. These findings suggest that the chemosensitizing effect of 10-G is mediated through inhibition of ADRB2/ERK signaling, which suppresses tumor growth and enhances paclitaxel sensitivity.

In vivo experiments further corroborated these observations, showing that 10-G, alone or in combination with paclitaxel, inhibited tumor growth without observable toxicity, confirming both efficacy and safety in a TNBC xenograft model.

Conclusion

This study demonstrates that 10-G enhances the sensitivity of TNBC cells to paclitaxel through modulation of the ADRB2/ERK signaling pathway. These findings position 10-G as a promising natural chemotherapeutic adjuvant and highlight ADRB2 as a potential therapeutic target. The results provide a foundation for developing ADRB2-targeted therapies with low toxicity derived from natural compounds. Future studies are warranted to evaluate the efficacy of 10-G across diverse TNBC patient populations.

References

1. Siegel RL, Miller KD, Fuchs HE, Jemal A. Cancer statistics, 2021. CA. 2021;71(1):7–33. doi:10.3322/caac.21654
2. Ahmad A. Breast cancer statistics: recent trends. Adv Exp Med Biol. 2019;1152:1–7. doi:10.1007/978-3-030-20301-6_1
3. Song X, Zhou Z, Li H, Xue Y, Lu X, Bahar I, et al. Pharmacologic suppression of B7-H4 glycosylation restores antitumor immunity in immune-cold breast cancers. Cancer Discov. 2020;10(12):1872-93. doi:10.1158/2159-8290.CD-20-0402. Epub 2020 Sep 16. PMID: 32938586; PMCID: PMC7710601.
4. Lebert JM, Lester R, Powell E, Seal M, McCarthy J. Advances in the systemic treatment of triple-negative breast cancer. Curr Oncol. 2018;25(1):S142–S50. doi:10.3747/co.25.3954
5. Won K-A, Spruck C. Triple-negative breast cancer therapy: current and future perspectives (Review). Int J Oncol. 2020;57(6):1245–61. doi:10.3892/ijo.2020.5135
6. Hu M-H, Wu T-Y, Huang Q, Jin G. New substituted quinoxalines inhibit triple-negative breast cancer by specifically downregulating the c-MYC transcription. Nucleic Acids Res. 2019;47(20):10529–42. doi:10.1093/nar/gkz835
7. Liu RH. Potential synergy of phytochemicals in cancer prevention: mechanism of action. J Nutr. 2004;134(12):3479S–85S. doi:10.1093/jn/134.12.3479S
8. Pezzani R, Salehi B, Vitalini S, Iriti M, Zuñiga FA, Sharifi-Rad J, et al. Synergistic effects of plant derivatives and conventional chemotherapeutic agents: an update on the cancer perspective. Medicina (Kaunas). 2019;55(4):110. doi:10.3390/medicina55040110. PMID: 30999703; PMCID: PMC6524059.
9. Hosseini-Zare MS, Sarhadi M, Zarei M, Thilagavathi R, Selvam C. Synergistic effects of curcumin and its analogs with other bioactive compounds: a comprehensive review. Eur J Med Chem. 2021;210:113072. doi:10.1016/j.ejmech.2020.113072
10. Li Y, Li S, Meng X, Gan R-Y, Zhang J-J, Li H-B. Dietary natural products for prevention and treatment of breast cancer. Nutrients. 2017;9(7):728. doi:10.3390/nu9070728
11. Yahyazadeh R, Baradaran Rahimi V, Yahyazadeh A, Mohajeri SA, Askari VR. Promising effects of gingerol against toxins: a review article. Biofactors. 2021;47(6):885–913. doi:10.1002/biof.1779
12. Zhang F, Thakur K, Hu F, Zhang J-G, Wei Z-J. Cross-talk between 10-gingerol and its anti-cancerous potential: a recent update. Food Funct. 2017;8(8):2635–49. doi:10.1039/C7FO00844A

13. Bernard MM, McConnery JR, Hoskin DW. [10]-Gingerol, a major phenolic constituent of ginger root, induces cell cycle arrest and apoptosis in triple-negative breast cancer cells. Exp Mol Pathol. 2017;102(2):370–6. doi:10.1016/j.yexmp.2017.03.006

14. Baptista Moreno Martin AC, Tomasin R, Luna-Dulcey L, Graminha AE, Araújo Naves M, Teles RH, et al. [10]-Gingerol improves doxorubicin anticancer activity and decreases its side effects in triple negative breast cancer models. Cellular Oncology. 2020;43(5):915-29.

15. Huang P, Zhou P, Liang Y, Wu J, Wu G, Xu R, et al. Exploring the molecular targets and mechanisms of [10]-Gingerol for treating triple-negative breast cancer using bioinformatics approaches, molecular docking, and in vivo experiments. Translational Cancer Research. 2021;10(11):4680.

16. Philipp M, Hein L. Adrenergic receptor knockout mice: distinct functions of 9 receptor subtypes. Pharmacol Ther. 2004;101(1):65–74. doi:10.1016/j.pharmthera.2003.10.004

17. Mele L, Del Vecchio V, Marampon F, Regad T, Wagner S, Mosca L, et al. β_2-AR blockade potentiates MEK1/2 inhibitor effect on HNSCC by regulating the Nrf2-mediated defense mechanism. Cell Death Dis. 2020;11(10):850. doi:10.1038/s41419-020-03056-x. PMID: 33051434; PMCID: PMC7555890.

18. Du Y, Yan T, Zhou L, Yin W, Lu J. A single-nucleotide polymorphism of the beta 2-adrenergic receptor gene can predict pathological complete response to taxane- and platinum-based neoadjuvant chemotherapy in breast cancer. Breast Cancer. 2018;10:201–6. doi:10.2147/BCTT.S189197

19. Kafetzopoulou LE, Boocock DJ, Dhondalay GKR, Powe DG, Ball GR. Biomarker identification in breast cancer: beta-adrenergic receptor signaling and pathways to therapeutic response. Comput Struct Biotechnol J. 2013;6:e201303003. doi:10.5936/csbj.201303003

20. Barron TI, Connolly RM, Sharp L, Bennett K, Visvanathan K. Beta blockers and breast cancer mortality: a population- based study. J Clin Oncol. 2011;29(19):2635–44. doi:10.1200/JCO.2010.33.5422

21. Haldar R, Shaashua L, Lavon H, Lyons YA, Zmora O, Sharon E, et al. Perioperative inhibition of β-adrenergic and COX2 signaling in a clinical trial in breast cancer patients improves tumor Ki-67 expression, serum cytokine levels, and PBMCs transcriptome. Brain Behav Immun. 2018;73:294-309. doi:10.1016/j.bbi.2018.05.014. Epub 2018 May 22. PMID: 29800703.

22. Wu FQ, Fang T, Yu LX, Lv GS, Lv HW, Liang D, et al. ADRB2 signaling promotes HCC progression and sorafenib resistance by inhibiting autophagic degradation of HIF1α. J Hepatol. 2016;65(2):314-24. doi:10.1016/j.jhep.2016.04.019. Epub 2016 May 3. PMID: 27154061.

23. Khatua B, El-Kurdi B, Patel K, Rood C, Noel P, Crowell M, et al. Adipose saturation reduces lipotoxic systemic inflammation and explains the obesity paradox. Sci Adv. 202;7(5):eabd6449. doi:10.1126/sciadv.abd6449. PMID: 33514548; PMCID: PMC7846167.

24. Lee SO, Li X, Hedrick E, Jin UH, Tjalkens RB, Backos DS, et al. Diindolylmethane analogs bind NR4A1 and are NR4A1 antagonists in colon cancer cells. Mol Endocrinol. 2014;28(10):1729-39. doi:10.1210/me.2014-1102. Epub 2014 Aug 6. PMID: 25099012; PMCID: PMC4179635.

25. Schvarcz CA, Danics L, Krenács T, Viana P, Béres R, Vancsik T, et al. Modulated electro-hyperthermia induces a prominent local stress response and growth inhibition in mouse breast cancer isografts. Cancers (Basel). 2021;13(7):1744. doi:10.3390/cancers13071744. PMID: 33917524; PMCID: PMC8038813.

26. Liang Y, Lv Z, Huang G, Qin J, Li H, Nong F, et al. Prognostic significance of abnormal matrix collagen remodeling in colorectal cancer based on histologic and bioinformatics analysis. Oncol Rep. 2020;44(4):1671-85. doi:10.3892/or.2020.7729. Epub 2020 Aug 11. PMID: 32945508; PMCID: PMC7448414.

27. Zheng Y, Dai Y, Liu W, Wang N, Cai Y, Wang S, et al. Astragaloside IV enhances taxol chemosensitivity of breast cancer via caveolin-1-targeting oxidant damage. J Cell Physiol. 2019;234(4):4277-90. doi:10.1002/jcp.27196. Epub 2018 Aug 26. PMID: 30146689.

28. Liu Q-G, Li Y-J YL, Yao L. Knockdown of AGR2 induces cell apoptosis and reduces chemotherapy resistance of pancreatic cancer cells with the involvement of ERK/AKT axis. Pancreatology. 2018;18(6):678–88. doi:10.1016/j.pan.2018.07.003

29. Yakisich JS, Azad N, Venkatadri R, Kulkarni Y, Wright C, Kaushik V, et al. Digitoxin and its synthetic analog MonoD have potent antiproliferative effects on lung cancer cells and potentiate the effects of hydroxyurea and paclitaxel. Oncol Rep. 2016;35(2):878-86. doi:10.3892/or.2015.4416. Epub 2015 Nov 12. PMID: 26573786; PMCID: PMC4689486.

30. Ediriweera MK, Moon JY, Nguyen YT-K, Cho SK. 10-Gingerol targets lipid rafts associated PI3K/Akt signaling in radio-resistant triple negative breast cancer cells. Molecules. 2020;25:14. doi:10.3390/molecules25143164

31. Zhang F, Thakur K, Hu F, Zhang J-G, Wei Z-J. 10-Gingerol, a phytochemical derivative from "tongling white ginger", inhibits cervical cancer: insights into the molecular mechanism and inhibitory targets. J Agric Food Chem. 2017;65(10):2089–99. doi:10.1021/acs.jafc.7b00095

32. Fuzer AM, Martin ACBM, Becceneri AB, da Silva JA, Vieira PC, Cominetti MR. [10]-Gingerol affects multiple metastatic processes and induces apoptosis in MDAMB- 231 breast tumor cells. Anticancer Agents Med Chem. 2019;19(5):645–54. doi:10.2174/1871520618666181029125607

33. Hopson MB, Lee S, Accordino M, Trivedi M, Maurer M, Crew KD, et al. Phase II study of propranolol feasibility with neoadjuvant chemotherapy in patients with newly diagnosed breast cancer. Breast Cancer Res Treat. 2021;188(2):427-32. doi:10.1007/s10549-021-06210-x. Epub 2021 Apr 10. PMID: 33837871.

34. Zhang X, Zhang Y, He Z, Yin K, Li B, Zhang L, et al. Chronic stress promotes gastric cancer progression and metastasis: an essential role for ADRB2. Cell Death Dis. 2019;10(11):788. doi:10.1038/s41419-019-2030-2. PMID: 31624248; PMCID: PMC6797812.

35. Tang J, Li Z, Lu L, Cho CH. β-Adrenergic system, a backstage manipulator regulating tumour progression and drug target in cancer therapy. Semin Cancer Biol. 2013;23(6Pt B):533–42. doi:10.1016/j.semcancer.2013.08.009

36. He Q, Xue S, Tan Y, Zhang L, Shao Q, Xing L, et al. Dual inhibition of Akt and ERK signaling induces cell senescence in triple-negative breast cancer. Cancer Lett. 2019;448:94-104. doi:10.1016/j.canlet.2019.02.004

37. Ahmed TA, Adamopoulos C, Karoulia Z, Wu X, Sachidanandam R, Aaronson SA, et al. SHP2 drives adaptive resistance to ERK signaling inhibition in molecularly defined subsets of ERK-dependent tumors. Cell Rep. 2019;26(1):65-78.e5. doi:10.1016/j.celrep.2018.12.013

38. Zhu S, Xu Y, Wang L, Liao S, Wang Y, Shi M, et al. Ceramide kinase mediates intrinsic resistance and inferior response to chemotherapy in triple-negative breast cancer by upregulating Ras/ERK and PI3K/Akt pathways. Cancer Cell Int. 2021;21(1):42. doi:10.1186/s12935-020-01735-5. PMID: 33430896; PMCID: PMC7802356.

39. Mukherjee B, Tiwari A, Palo A, Pattnaik N, Samantara S, Dixit M. Reduced expression of FRG1 facilitates breast cancer progression via GM-CSF/MEK-ERK axis by abating FRG1 mediated transcriptional repression of GM-CSF. Cell Death Discov. 2022;8(1):442. doi:10.1038/s41420-022-01240-w

40. Xie WY, He RH, Zhang J, He YJ, Wan Z, Zhou CF, et al. β-blockers inhibit the viability of breast cancer cells by regulating the ERK/COX-2 signaling pathway and the drug response is affected by ADRB2 single-nucleotide polymorphisms. Oncol Rep. 2019;41(1):341-50. doi:10.3892/or.2018.6830. Epub 2018 Oct 29. PMID: 30542705.

41. Lin H, Hu B, He X, Mao J, Wang Y, Wang J, et al. Overcoming Taxol-resistance in A549 cells: a comprehensive strategy of targeting P-gp transporter, AKT/ERK pathways, and cytochrome P450 enzyme CYP1B1 by 4-hydroxyemodin. Biochem Pharmacol. 2020;171:113733. doi:10.1016/j.bcp.2019.113733. Epub 2019 Nov 26. PMID: 31783010.

42. Dong Y, Ma Y, Li X, Wang F, Zhang Y. ERK-peptide-inhibitor-modified ferritin enhanced the therapeutic effects of paclitaxel in cancer cells and spheroids. Mol Pharm. 2021;18(9):3365–77. doi:10.1021/acs.molpharmaceut.1c00303

43. Ryu MJ, Chung HS. [10]-Gingerol induces mitochondrial apoptosis through activation of MAPK pathway in HCT116 human colon cancer cells. In Vitro Cell Dev Biol Anim. 2015;51(1):92–101. doi:10.1007/s11626-014-9806-6